Progress In Electromagnetics Research Letters, Vol. 36, 181–190, 2013

A COMPACT Ka-BAND BROADBAND WAVEGUIDE-BASED TRAVELING-WAVE SPATIAL POWER COMBINER WITH LOW LOSS SYMMETRIC COUPLING STRUCTURE

Zhiyong Kang, Qingxin Chu*, and Qiongsen Wu

School of Electronic and Information Engineering, South China University of Technology, Guangzhou, China

Abstract—A compact Ka-band broadband waveguide-based traveling-wave spatial power combiner is presented. The low loss micro-strip probes are symmetrically inserted into both broadwalls of waveguide, quadrupling the coupling ways but the insertion loss increases little. The measured 16 dB return-loss bandwidth of the eight-way back-to-back structure is from 30 GHz to 39.4 GHz (more than 25%) and the insertion loss is less than 1 dB, which predicts the power-combining efficiency is higher than 90%.

1. INTRODUCTION

It is necessary to combine power from multiple devices to obtain the desired power levels because the output power from an individual solid-state device is often not enough at millimeter-wave frequencies [1–10]. Planar divider/combiner based on Wilkinson types offer noticeable power loss at millimeter frequencies. On the contrary, waveguide-based power divider/combiner has the characteristics of low loss and good heat sinking. The waveguide-based traveling-wave power combining technique, where the coupling units are coupled along the longitudinal direction of the waveguide allowing combining more solid-state devices at millimeter frequencies [3], is widely studied [4–6].

Some excellent works have been done on the traveling-wave power combiner. An $N = 8$ traveling-wave power combiner using a slotted waveguide was proposed at Ka-band [2]. The structure had a bandwidth from 31.8 GHz to 35 GHz with the combining efficiency of 80%. A planar compatible traveling-wave power divider/combiner

Received 13 November 2012, Accepted 17 December 2012, Scheduled 21 December 2012
* Corresponding author: Qingxin Chu (qxchu@scut.edu.cn).

structure at X-band was presented [6]. The $N = 4$ structure exhibited the bandwidth of 15% and the power combining efficiency of approximately 80%. Some challenges of the traveling-wave combining technology are as follows: the contradiction between the multi-ways and the bandwidth; low combining efficiency because the insertion loss increases with the coupled stages added.

In this paper, a compact waveguide-based multi-way traveling-wave power combiner is presented, which combines the traveling-wave power combining technique and spatial power combining technique. In [7], the coupling ways are doubled by using dual-probe structure inserted into one broadwall of the waveguide. Here, the combining ways are quadrupled but the insertion loss increases little by inserting the dual-probe on both broadwalls of the waveguide. Compare with paper [7], the combing ways are doubled in the situation of the same power dividing stages and an E-T junction is needed. Because the E-T junction is needed additionally, the insertion loss of the proposed structure is the same as the structure proposed in [7] in the case of eight-way power combiner. However, when the combining ways increased, the insertion loss is less and the design process is simple compared to the technique proposed in [7]. The structure has potential to realize more coupling ways with high power combining efficiency at millimeter and even higher frequencies.

2. DESIGN APPROACH

The structure of the eight-way back-to-back combiner is shown in Figure 1, which can be composed into two parts: an eight-way power

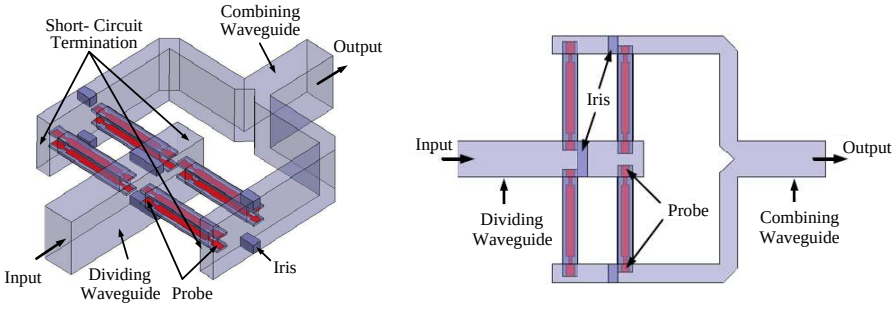

Figure 1. The structure of the two-stage eight-way combiner. (a) The module of the proposed combiner. (b) Top view of the proposed structure.

divider and an E-T junction. Firstly, a series of planar probes are designed to pick off the equal power traveling from the input of the dividing waveguide. Each probe then directs the coupling power along a transmission line to be amplified by an active circuit (not shown in the picture) and then recombined via a planar probe first in the half height waveguides (The width of the waveguide is the same as that of a standard waveguide, while the height is half of a standard one.). At last the power from the reduced height waveguides is combined via an E-T junction to the standard output waveguide. For the symmetry of the structure, the input and output ports can be swapped.

As shown in Figure 1, the design process of the power combiner is decomposed into two steps: a two-stage eight-way power divider and an E-T junction designing.

2.1. Design a Two-stage Eight-way Power Divider

The method of images is used to simplify design process of the symmetrical structure. Electric field of the TE_{10} mode of the rectangle waveguide is showed in Figure 2. Figure 3 is the mirror electric field with the boundary condition of perfect electric conductor (PEC) and perfect magnetic conductor (PMC). Therefore, the eight-way power

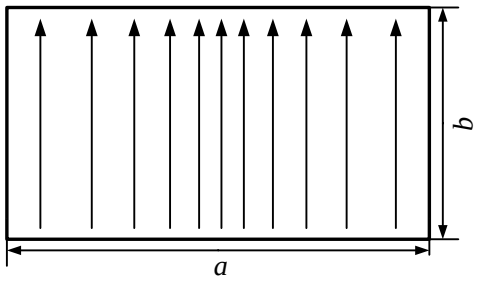

Figure 2. Electric field of the TE_{10} mode of the rectangle waveguide.

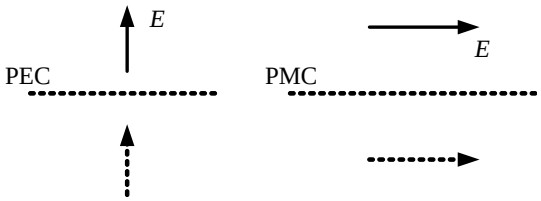

Figure 3. Mirror electric field with the boundary condition of PEC and PMC.

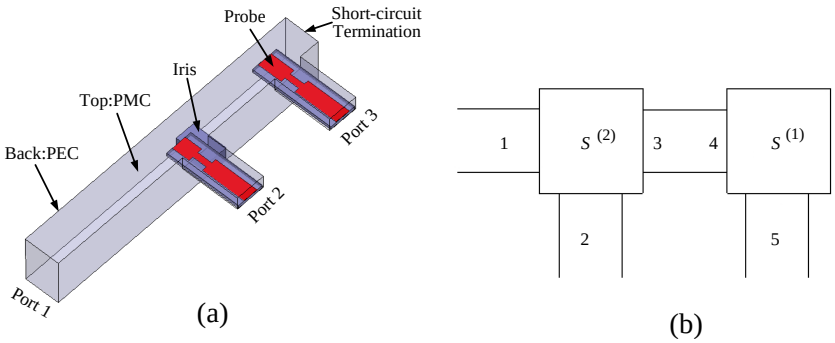

Figure 4. The two-way traveling-wave power divider.

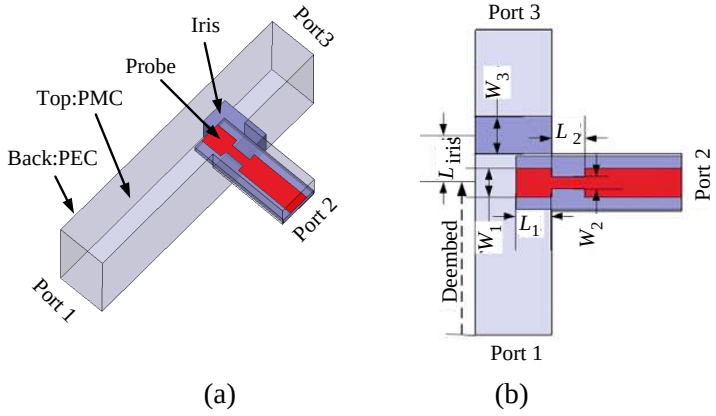

Figure 5. Single waveguide-to-microstrip coupler.

divider can be simplified into a two-way traveling-wave power divider with appropriate boundary condition of PEC and PMC, as shown in Figure 4(a). The design process and simulation time are reduced by using the symmetric method.

The design of the traveling-wave power divider is approached by decomposing the structure into a series of three-port components, apart from the last probe in the divider which is two-port component for the existence of a short-circuit waveguide termination. Figure 5 is a sketch of one of the three-port components, which is composed of a microstrip probe and a metallic iris whose function is to bring the input conductance of the three-port component to unity and to cancel any residual susceptance [6]. The traveling-wave nature requires reflectionless of the decomposed units and every probe receiving equal power

that travels from the input of the dividing waveguide. Therefore, the scattering matrixes for the ith power-dividing stage are

$$\left|S_{11}^{(i)}\right|^2 = 0 \tag{1}$$

$$\left|S_{21}^{(i)}\right|^2 = \frac{1}{i} \tag{2}$$

$$\left|S_{31}^{(i)}\right|^2 = \frac{i-1}{i} \tag{3}$$

Ports 1 and 3 are the waveguide ports, while port 2 is the micro-strip port (as shown in Figure 3(a)). i is the sequence number of the ith probe measured from the last probe of the divider ($i = 1, 2, 3, \ldots, N$). In this case, $i = 1, 2$.

The equivalent circuit concept is used [4] to design the decomposed components. Assume the equivalent admittance of the micro-strip probe is $Y_{pi} = g_{pi} + jb_{pi}$, the equivalent admittance looking toward the metallic iris at micro-strip probe is $Y_i = g_i + jb_i$, where all the conductance and susceptance are normalized by the characteristic admittance of the waveguide (Y_0). In order to realize the request of (1)–(3), the admittances of the ith probe and metallic iris are given as:

$$g_{pi} = 1/i \tag{4}$$

$$g_i = (i-1)/i \tag{5}$$

$$Y_{pi} + Y_i = 1 \tag{6}$$

Figure 5(b) presents the key deembedded design dimensions of the ith three-port component (the iris height (D) is not shown). L_{iris} is the distance from the center of probe to the center of the iris. The high-impedance micro-strip is used to achieve impedance match and flat coupling coefficients in wide frequencies range [11]. For the $g_{p1} = 1$ probe, the iris is replaced by a short-circuit waveguide termination with a suitable distance to the center of the probe. Using Ansoft Corporations' commercial software tool High Frequency Structure Simulator (HFSS), the deembedded S-parameters of the probe and iris are simulated separately. Then the admittances of the probe and iris can be calculated from the deembedded S-parameters as proposed in [6]. After the Y_{pi} and Y_i are simulated respectively by HFSS satisfying (4)–(6), the micro-strip probe and the iris are combined to be a three-port component with reflection-less and specific coupling coefficient. Figure 6 is the reflection and power dividing coefficients of $g_{p2} = 0.5$ component simulated by HFSS. From 30 GHz to 40 GHz, the reflection is less than -18 dB and the deviation of power dividing coefficients is less than ± 0.3 dB.

When the divided units are cascaded to be a two-way power divider, the reflected wave caused by probe units may affect each other

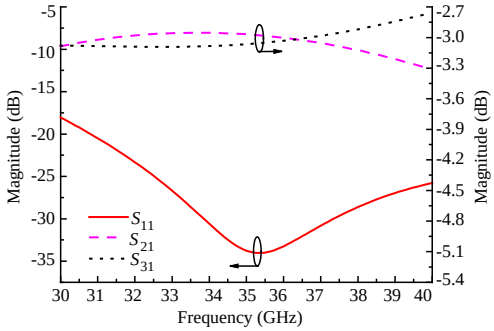

Figure 6. Reflection and power dividing coefficients of $g_{p2} = 0.5$.

and reduce the bandwidth. Therefore, the distance of between the units is another factor need to be considered. Figure 4(b) is the sketch of a top-level signal flow diagram of the $N = 2$ power divider, the scattering matrixes of the two-way power divider are given as:

$$S'_{11} = S_{11} + \frac{S_{31}S_{43}S_{44}S_{34}S_{13}}{1 - S_{33}S_{44}S_{43}S_{34}} \approx S_{11} + S_{31}S_{43}S_{44}S_{34}S_{13} \quad (7)$$

$$S'_{21} = S_{21} + \frac{S_{31}S_{43}S_{44}S_{34}S_{23}}{1 - S_{33}S_{43}S_{34}S_{44}} \approx S_{21} + S_{31}S_{43}S_{44}S_{34}S_{23} \quad (8)$$

$$S'_{51} = \frac{S_{31}S_{43}S_{54}}{1 - S_{33}S_{43}S_{44}S_{34}} \approx S_{31}S_{43}S_{54} \quad (9)$$

In the expressions, the scattering parameters without single quotes are the original of single divided unit. When the probe units are connected, the scattering parameters with single quotes are the scattering parameters of the divider. It is assumed that $S_{33}S_{44} \ll 1$ in the expressions.

As seen from (7)–(9), the full divider structure's scattering parameters S'_{11}, S'_{21} are determined by two monomials. Take S'_{21} for example, to obtain a wider bandwidth of S'_{21}, firstly S_{21} should be designed well, then adjust $S_{31}S_{43}S_{44}S_{34}S_{23}$ to increase or decrease S_{21}. The $S_{43}S_{34}$ can be adjusted easily by adjusting the distance between the probes. Some design guidelines for achieving broadband characteristic are presented below:

(1) Improve the single-stage coupling structure to get a flat amplitude-frequency characteristic of S_{21} and low return loss of the input waveguide over a broad band.

(2) Optimize the distance between stages to reduce the amplitude imbalance of S'_{n1} and obtain low reflection.

The distance of the adjacent coupler components is optimized as

5.4 mm for the perfect broadband matching. The optimized dimensions of the micro-strip probes and the iris are listed in Table 1 (the iris is replaced by a short-circuit termination with a distance of 1.8 mm to the center of the $g_{p1} = 1$ probe).

When the two-way power divider with suitable boundary condition is simulated, the two-stage eight-way power divider is easily achieved for the symmetry of the structure. Figure 7 shows the simulated reflection and dividing coefficients of the eight-way power divider, where the reflection is less than -19 dB and the deviation of power dividing coefficients is less than ± 0.7 dB in the range of 30–40 GHz.

2.2. Design of E-T Junction

The 3 dB E-T junction is used to combine the power from two half height waveguides to the standard output waveguide (as shown in Figure 1). The characteristic impedance of the waveguide is given when the TE_{10} mode is considered:

$$Z_0 \propto \frac{b}{a} \cdot \frac{\sqrt{u/\varepsilon}}{\sqrt{1-(\lambda/2a)^2}} \tag{10}$$

Therefore, the two input half height waveguides are nature

Table 1. Probe and iris dimensions (in mm).

g_p	W_1	L_1	W_2	L_2	L_{iris}	W_3	D
1	0.76	1.23	0.3	0.75	N/A	N/A	N/A
1/2	0.76	0.84	0.3	0.75	1.2	1	1.18

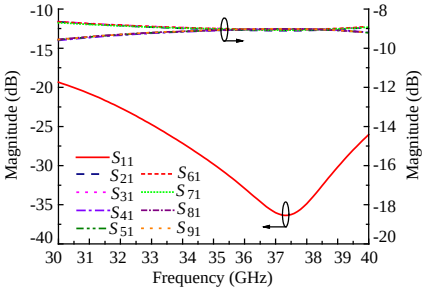

Figure 7. Reflection and power dividing coefficients of the eight-way power divider.

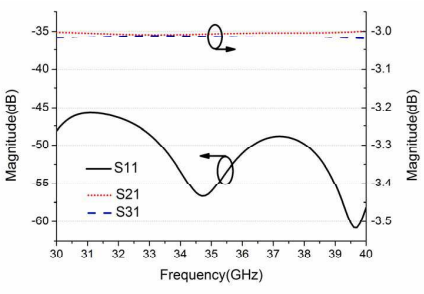

Figure 8. The S-parameter of the E-T junction.

matched to the standard output waveguide. The residual susceptance is canceled by a corner cut. The S-parameter of the E-T junction is showed in Figure 8, which presents the good match and equal power dividing.

3. SIMULATED RESULTS

When the eight-way power divider and the 3 dB E-T junction have been designed, the 3 dB E-T junction combines the power from two half height waveguides to form the eight-way power combiner (as shown in Figure 1). Finally, the back-to-back structure of the eight-way traveling-wave spatial power combiner has been fabricated and measured. Figure 9 shows the two half fabricated structures, which are combined to be a power combiner. The input/output waveguide

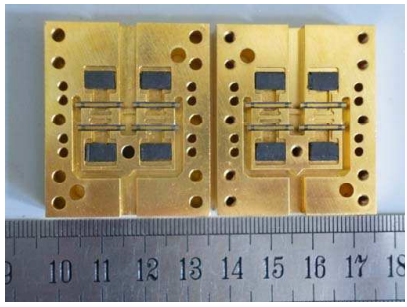

Figure 9. The two half fabricated power combiners.

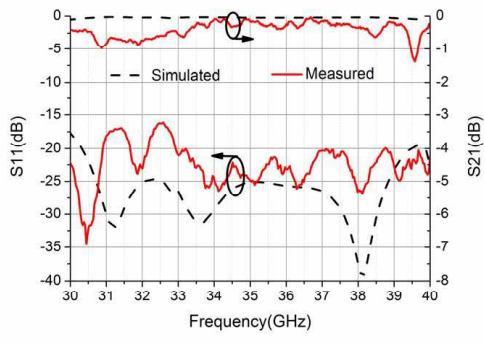

Figure 10. The comparison of simulated and measured S-parameters of the back-to-back structure.

is the standard WR28 rectangular waveguide, and the substrate of the micro-strip is 0.254 mm thick Rogers RT/duroid 5880 material (relative permittivity of 2.2). The measure is using Agilent 5230A vector network analyzer by taking Thru-Reflect Line calibration technique. Figure 10 is the comparison of simulated and measured reflection of the input and insertion loss of the back-to-back structure, the measured return loss is greater than 16 dB and insertion loss is less than 1 dB over 30–39.4 GHz. The measured results validate the effectiveness of the design method. The reason of difference between the simulated and measured data is that the micro-strip is placed by hand.

4. CONCLUSION

A compact broadband waveguide-based traveling-wave spatial power combiner with low loss symmetric coupling structure at *Ka*-band has been presented in this paper. The coupling ways were quadrupled but the insertion loss increased little by inserting the dual-probe into both broad-walls of the waveguide. A two-stage eight-way combiner has been designed, fabricated and measured. From 30 GHz to 39.4 GHz, the measured return loss of the back-to-back structure was greater than 16 dB and insertion loss was less than 1 dB, which predicts high power combining efficiency. The passive power divider/combiner demonstrates the characters of wide bandwidth and low insertion loss, which is suitable for millimeter wave and even higher frequencies power combiner.

ACKNOWLEDGMENT

This work was supported by the National Natural Science Foundation of China (61171029) and Guangzhou Science and Technology Project (12C42081659).

REFERENCES

1. Chang, K. and C. Sun, "Millimeter-wave power-combining techniques," *IEEE Trans. Microwave Theory & Tech.*, Vol. 31, No. 2, 91–107, Feb. 1983.
2. Jiang, X., S. C. Oritiz, and A. Mortazawi, "A *Ka*-band power amplifier based on the traveling-wave power-dividing/combining slotted-waveguide circuit," *IEEE Trans. Microwave Theory & Tech.*, Vol. 52, No. 2, 633–639, Feb. 2004.

3. Shapiro, E. S., J. Xu, A. S. Nagra, F. Williams, Jr., U. K. Mishra, and R. A. York, "A high-efficiency traveling-wave power amplifier topology using improved power-combining techniques," *IEEE Microwave Guide Wave Lett.*, Vol. 8, No. 3, 133–1356, Mar. 1998.
4. Sanada, A., K. Fukui, S. Nogi, and M. Sanagi, "Traveling-wave microwave power divider composed of reflectionless dividing units," *IEEE Trans. Microwave Theory & Tech.*, Vol. 43, No. 1, 14–20, Jan. 1995.
5. Jiang, X., L. Liu, S. C. Ortiz, R. Bashirullah, and A. Mortazawi, "A Ka-band power amplifier based on a low-profile slotted-waveguide power-combining/dividing circuit," *IEEE Trans. Microwave Theory & Tech.*, Vol. 51, No. 1, 144–147, Jan. 2003.
6. Li, L. A., B. J. Hilliard, J. R. Shafer, J. Daggett, E. J. Dickman, and J. P. Becker, "A planar compatible traveling-wave waveguide-based power divider/combiner," *IEEE Trans. Microwave Theory & Tech.*, Vol. 56, No. 8, 1889–1898, Aug. 2008.
7. Kang, Y. Z., Q. X. Chu, and Q. S. Wu, "A Ka-band waveguide-based traveling-wave spatial power divider/combiner," *IEEE International Conference on Microwave and Millimeter Wave Technology (ICMMT)*, Vol. 5, 1–4, 2012.
8. Li, X.-Q., Q.-X. Liu, and J.-Q. Zhang, "A high-power low-loss multiport radial waveguide power divider," *Progress In Electromagnetics Research Letters*, Vol. 31, 189–198, 2012.
9. Huang, S., X. Xie, and B. Yan, "K band Wilkinson power divider based on a taper equation," *Progress In Electromagnetics Research Letters*, Vol. 27, 75–83, 2011.
10. Olvera Cervantes, J. L., A. Corona-Chavez, R. Chavez-Perez, H. Lobato-Morales, J.-R. Ortega-Solis, and J.-L. Medina-Monroy, "A wideband quadrature power divider/combiner and its application to an improved balanced amplifier," *Progress In Electromagnetics Research C*, Vol. 34, 29–39, 2013.
11. Shih, Y. C., T. N. Ton, and L. Q. Bui, "Waveguide-to-microstrip transitions for millimeter-wave applications," *IEEE MTT-S Int. Microwave Symp. Dig.*, Vol. 1, 473–475, May 2002.